The Stellar IMF from Turbulent Fragmentation

Paolo Padoan[1]

Jet Propulsion Laboratory, California Institute of Technology, MS 169-506, 4800 Oak Grove Drive, Pasadena, CA 91109

Åke Nordlund[2]

Astronomical Observatory and Theoretical Astrophysics Center, Juliane Maries Vej 30, DK-2100 Copenhagen, Denmark, aake@astro.ku.dk

Received _____; accepted _____

[1]padoan@ted.jpl.nasa.gov

[2]aake@astro.ku.dk

ABSTRACT

The morphology and kinematics of molecular clouds (MCs) are best explained as the consequence of super–sonic turbulence. Super–sonic turbulence fragments MCs into dense sheets, filaments and cores and large low density "voids", via the action of highly radiative shocks. We refer to this process as *turbulent fragmentation.*

In this work we derive the mass distribution of gravitationally unstable cores generated by the process of turbulent fragmentation. The mass distribution above one solar mass depends primarily on the power spectrum of the turbulent flow and on the jump conditions for isothermal shocks in a magnetized gas. For a power spectrum index $\beta = -1.74$, consistent with Larson's velocity dispersion–size relation as well as with new numerical and analytic results on super–sonic turbulence, we obtain a power law mass distribution of dense cores with a slope equal to $3/(4-\beta) = 1.33$, consistent with the slope of the stellar IMF. Below one solar mass, the mass distribution flattens and turns around at a fraction of a solar mass, as observed for the stellar IMF in a number of stellar clusters, because only the densest cores are gravitationally unstable. The mass distribution at low masses is determined by the probability distribution of the gas density that is known to be approximately Log–Normal for an isothermal turbulent gas. The intermittent nature of the turbulent density distribution is responsible for the existence of a significant number of small collapsing cores, even of sub–stellar mass.

Since turbulent fragmentation is unavoidable in super–sonically turbulent molecular clouds, and given the success of the present model to predict the observed shape of the stellar IMF, we conclude that turbulent fragmentation is essential to the origin of the stellar IMF.

Subject headings: turbulence – ISM: kinematics and dynamics – stars: formation – stars: mass function

1. Introduction

The process of star formation, particularly the origin of the stellar initial mass function (IMF), is a fundamental problem in astrophysics. Photometric properties and chemical evolution of galaxies depend on their stellar content. More importantly, the process of galaxy formation cannot be described independently of the process of star formation, since galaxies are partly made of stars. Stars are also an important energy source for the interstellar medium of galaxies. Star formation is one of the most challenging problems in modern cosmology.

Stars are formed in molecular clouds (MCs), which have been the focus of the research on star formation for more than two decades. Currently, there is no generally accepted theory of star formation, capable of predicting the star formation rate and the stellar IMF based on the physical properties of MCs. This is hardly surprising because turbulent motion is ubiquitously observed in MCs, and the physics of turbulence is poorly understood, due to the great mathematical complexity of the fluid equations. Magnetic field, self–gravity and high Mach numbers further increase the complexity.

The steady growth of computer performance has now made large three–dimensional numerical simulations of super–sonic magneto-hydrodynamic (MHD) turbulence feasible (Padoan & Nordlund 1997, 1999; Stone, Ostriker & Gammie 1998; MacLow et al. 1998; Padoan, Zweibel & Nordlund 2000; Klessen, Heitsch & Mac Low 2000; Mac Low & Ossenkopf 2000; Ostriker, Stone & Gammie 2000; Heitsch, Mac Low & Klessen 2000; Padoan et al. 2001a,b). Comparisons of numerical experiments with observational data have shown that super–sonic turbulence can explain the morphology and kinematics of MCs, and the formation of dense cores, provided that the motions are also super-Alfvénic (Padoan, Jones & Nordlund 1997; Padoan et al. 1998; Padoan & Nordlund 1997, 1999; Padoan et al. 1999; Padoan, Rosolowsky & Goodman 2001; Padoan et al. 2001a, b). We refer to this process of formation of dense cores in MCs by super–sonic turbulence as *turbulent fragmentation*. Since protostars evolve from the collapse of gravitationally unstable cores in MCs, even the stellar IMF could then be the result of turbulent fragmentation, with the power law shape of the IMF ultimately being the consequence of the self–similar nature of turbulence.

In this paper we do not use these increasingly sophisticated numerical simulations directly, but instead develop an analytic model. The assumptions of the model are *inspired* by the qualitative properties of the numerical model, but the current work does not *depend* on any particular set of numerical models or results.

Previous analytic models by Larson (1992), Henriksen (1986, 1991) and Elmegreen (1997, 1999, 2000b) have derived the stellar IMF on the basis of the self–similar structure of MCs. Larson, assuming

one dimensional accretion, predicted a rather steep IMF slope, equal to the MC fractal dimension, while Henriksen found the IMF slope to depend on both the MC fractal dimension and the relation between density and linear size for structures inside MCs. Elmegreen pointed out that the IMF that results from random sampling of a self–similar cloud has an exponent $x = 1$ (Salpeter $x = 1.35$), independent of the cloud fractal dimension. In Elmegreen's model the IMF is steeper than $x = 1$ because the random sampling rate is assumed to be proportional to the square root of density, and because of "mass competition".

These models are based on assumptions about the cloud geometry justified by the apparent fractal structure of MCs (Beech 1987; Bazell & Désert 1988, Scalo 1990; Dickman, Horvath & Margulis 1990; Falgarone, Phillips & Walker 1991; Zimmermann, Stutzki & Winnewisser 1992; Henriksen 1991; Hetem & Lepine 1993; Vogelaar & Wakker 1994; Elmegreen & Falgarone 1996), but the processes responsible for generating the assumed geometry are not discussed in detail.

In a previous attempt to relate the stellar IMF to the physical properties of super–sonic turbulence (Padoan, Nordlund & Jones 1997), we obtained the distribution of the local Jeans' mass in super–sonic isothermal turbulence, from the probability distribution of the gas density. That work also provides a prediction for the stellar IMF, by identifying each local Jeans' mass with a protostar. Although the prediction of the lower mass cutoff and the low mass portion of the IMF might be roughly correct, this model under–estimates the number of massive stars relative to low mass stars (as any other Log-Normal IMF). The main reason, as pointed out by Scalo et al. (1998), is the unphysical assumption that the most massive stars originate from gas at relatively low density including only a small fraction of the total mass.

In the present work we consider specific properties of MC turbulence and their consequences for the formation of protostellar cores. In particular, we i) assume approximate self–similarity of the super–sonic and super–Alfvénic velocity field, expressed by a power law shape of the power spectrum of turbulence, and ii) assume that the jump conditions for isothermal MHD shocks determine the scaling of the typical size of protostellar cores. Based on these fundamental assumptions, we are able to derive a power law mass distribution of gravitationally unstable cores with the same slope as the Salpeter stellar IMF (Salpeter 1955), without a dependence on any free parameters. In order to derive the mass distribution of gravitationally unstable cores below one solar mass we also make use of the Probability Density Function (PDF) of the mass density in super–sonic turbulence, following Padoan, Nordlund & Jones (1997).

The formation of dense cores and the relation between the size of cores and the thickness of the postshock gas are discussed in the next section. In § 3 the power spectrum of super–sonic turbulence is

discussed. Results on the PDF of the gas density in super–sonic turbulence are summarized in § 4. The mass distribution of dense cores formed by the process of turbulent fragmentation is derived in § 5, and the mass distribution of gravitationally unstable cores is computed in § 6. The relevance of these results for the origin of the stellar IMF is discussed in § 7 and 8. Conclusions are summarized in § 9.

2. The Origin of Dense Cores in Super–Sonic Turbulence

The qualitative properties of the local density maxima that form in super–sonic turbulence follow from first principles and numerical experiments have confirmed such properties.

Dense cores are formed in roughly isothermal super–sonic turbulent flows as the densest parts of sheets or filaments of shocked gas. In a super–sonic turbulent flow, density fluctuations are present over a large range of scales. As a result, the surfaces of postshock sheets are never perfectly plane and smooth, but rather curved and corrugated. A corrugation in the direction of the preshock velocity corresponds to a local maximum in the value of the shock velocity, which advects the flow beyond the average plane of the shock. Because the postshock gas density grows with the Alfvénic Mach number of the shock (see below), the densest postshock gas in a sheet can be found in corrugations, due to the large velocity, or in regions where the magnetic field components parallel to the plane of the shock are relatively weak prior to the compression.

Since dense cores are formed as the densest parts of postshock sheets, their typical size is comparable to the sheet thickness, λ. Assuming that the magnetic pressure in the postshock gas exceeds the thermal pressure (this is the case for a large range of values of the preshock magnetic field strength, even when the flow is super–Alfvénic), the isothermal shock jump conditions are:

$$\frac{\rho_1}{\rho_0} \approx \mathcal{M}_a \tag{1}$$

$$\frac{\lambda}{L} \approx \mathcal{M}_a^{-1} \tag{2}$$

$$\frac{B_1}{B_0} \approx \mathcal{M}_a \tag{3}$$

where ρ_0, B_0 and ρ_1, B_1 are the values of the gas density and magnetic field strength before and after the shocks, respectively. L is the linear extension of the gas before the shock (measured in the direction perpendicular to the shock surface) and λ is the thickness of the postshock gas. $\mathcal{M}_a$ is the Alfvénic Mach number of the shock, that is the ratio of the flow velocity and the Alfvén velocity measured in the preshock

gas:

$$\mathcal{M}_a = \frac{v}{v_a} = \frac{v}{B_0/\sqrt{4\pi\rho_0}} \tag{4}$$

Here the relevant magnetic field components are the ones parallel to the shock surface, because the perpendicular component does not provide pressure support against the compression and it is not amplified by the compression. Since only the parallel components of **B** are amplified, the field in the postshock sheets is nearly parallel to the sheet surface, and elongated in the direction of dense filaments (real ones, or two–dimensional sections of sheets). Since dense cores are formed predominantly in corrugations of sheets, the magnetic field within dense cores can occasionally show a strong curvature, depending on the orientation relative to the line of sight. This may considerably complicate the interpretation of dust polarization measurements (Ward–Thompson et al. 2000) and should be taken into account.

3. The Power Spectrum of Super–Sonic Turbulence

The power spectrum of turbulence in the inertial range (below the energy injection scale and above the dissipation scale) may be assumed to be a power law,

$$E(k) \propto k^{-\beta}, \tag{5}$$

where k is the wave–number, and the spectral index is $\beta \approx 5/3$ for incompressible turbulence (Kolmogorov power spectrum) (Kolmogorov 1941), and $\beta \approx 2$ for pressureless turbulence (Burgers power spectrum) (Burgers 1974; Gotoh & Kraichnan 1993). The $\beta = 2$ power spectrum has often been assumed to be the correct power spectrum of super-sonic turbulence, at least for the compressional component of the velocity field.

The purpose of the present work is primarily that of establishing analytically a relation between the power spectrum of turbulence and the stellar IMF and we only need to assume that the power spectrum is a power law in the inertial range. Our analytic model does not assume a specific value of the spectral index, as obtained for example in numerical simulations. However, the predictions of our analytic model will be tested using the power spectrum of super–sonic turbulence computed from numerical simulations or estimated from observational data. For that reason we briefly summarize in this section some numerical and observational results.

3.1. The Power Spectrum in Numerical Simulations

The most detailed study of the power spectrum of numerical compressible turbulence has been presented by Porter, Pouquet & Woodward (1992, 1994) and Porter, Woodward & Pouquet (1998). From the 1992 paper to the 1998 paper the largest numerical resolution increased from 256^3 to 1024^3. These works are limited to decaying turbulence, with Mach numbers close to unity initially, and below unity at later times. The runs are therefore sub–sonic, except for an initial period of time. A magnetic field is not included.

The velocity field is usually decomposed into its solenoidal $\mathbf{v}^s$ and compressional $\mathbf{v}^c$ components as $\mathbf{v} = \mathbf{v}^s + \mathbf{v}^c$ with $\nabla \cdot \mathbf{v}^s = 0$ and $\nabla \times \mathbf{v}^c = 0$. The velocity Fourier spectrum, $E(k)$, is also separated into its solenoidal and compressional parts: $E(k) = E^s(k) + E^c(k)$.

Porter, Pouquet & Woodward (1992) found that the compressional modes have a power spectrum $E^c(k) \propto k^{-2}$, and the solenoidal modes $E^s(k) \propto k^{-1}$. In the later works, after the larger numerical resolution runs were performed, the same authors concluded instead that both compressional and solenoidal modes develop a Kolmogorov power spectrum, $E^c(k) \propto E^s(k) \propto k^{-5/3}$, with $E^c/E^s \approx 0.15$ (Porter, Pouquet & Woodward 1994; Porter, Woodward & Pouquet 1998). This conclusion is not strongly supported by the plots of power spectra presented by the authors, since the largest resolution runs (512^3 and 1024^3) are consistent with a Kolmogorov power spectrum for the solenoidal modes only over a very limited range of wave–numbers, approximately $4 < k < 10$. At larger wave–numbers, the power spectrum is flatter, approximately $E^s(k) \propto k^{-1}$. An interpretation of the shallower power spectrum of solenoidal modes at large wave numbers is provided, in terms of a "near dissipation range". The discrepancy between the steeper (Burgers) power spectrum of compressional modes in the early 256^3 runs (Porter, Pouquet & Woodward 1992) and the Kolmogorov power spectrum in the latest 256^3 runs (Porter, Pouquet & Woodward 1994; Porter, Woodward & Pouquet 1998) is not discussed.

We have recently started to perform a large number of numerical experiments with the purpose of computing the spectral index of the inertial range of driven super–sonic MHD turbulence as a function of the sonic and Alfvénic rms Mach numbers of the flow. The experiments use an isothermal equation of state, uniform initial density and magnetic fields, random initial velocity and random large scale forcing (both solenoidal), as described in previous works (Padoan et al. 1998; Padoan & Nordlund 1999; Padoan, Zweibel & Nordlund 2000). The results of these new experiments will be reported and discussed elsewhere (Jimenez, Padoan & Nordlund 2001). Preliminary numerical results are reported in Boldyrev, Nordlund

& Padoan (2001), where the numerical scaling relations are also predicted on the basis of a new analytic model of super–sonic turbulence. A power spectrum intermediate between the Burgers and the Kolmogorov power spectra is found, $E(k) \propto k^{-1.74}$.

3.2. The Power Spectrum from Observational Data

The observed velocity dispersion–size Larson relation (Larson 1979, 1981), $\Delta v \propto L^{\alpha}$, should reflect the power spectrum of turbulence in the interstellar medium ($\alpha = (\beta - 1)/2$), although it is often obtained from a combination of different clouds and cores inside the same cloud, or even different molecular transitions (see Goodman et al. 1998 for a discussion of the line width–size relation). Larson finds $\alpha = 0.37$ in the range of scales $1 < L < 1000$ pc (Larson 1979); and $\alpha = 0.38$ in the range of scales $0.1 < L < 100$ pc (Larson 1981); Leung, Kutner & Mead (1982) obtain $\alpha = 0.48$ for $0.2 < L < 4$ pc; Myers (1983) gets $\alpha = 0.5$ for $0.04 < L < 10$ pc; Sanders, Scoville & Solomon (1985) find an unusually large value $\alpha = 0.62$ for $20 < L < 100$ pc, which they use to rule out any relation between a turbulent power spectrum and the line width–size relation; Dame et al. (1986) obtain $\alpha = 0.5$ for $10 < L < 150$ pc; finally Falgarone, Puget & Pérault (1992) use a compilation of data from the literature together with their own new data, in order to sample a very large range of scales, $0.01 < L < 100$ pc, and include also a significant number of unbound objects (velocity dispersion larger than the virial velocity), which are usually not included in earlier studies. They find a correlation consistent with $\alpha = 0.4$, and a very large total scatter of almost one order of magnitude in line width. The value $\alpha = 0.4$ for the exponent of the line width–size relation corresponds to a power spectrum of turbulence $\propto k^{-1.8}$.

Miesch & Bally (1994) have estimated the power spectrum of turbulence in molecular clouds by computing the autocorrelation and structure functions of emission line centroid velocities. Their results correspond to an average exponent for the line width–velocity relation $\alpha = 0.43$, or a power spectrum with $\beta = 1.86$. Previous attempts to measure the power spectrum of turbulence in molecular clouds with the same method had provided much shallower spectra (Kleiner & Dickman 1987; Hobson 1992).

A new method to estimate the power spectrum of turbulence in molecular clouds has also been recently proposed by Brunt & Heyer (2000), using the Principal Component Analysis by Heyer & Schloerb (1997). The method has already been applied to 23 molecular clouds in the outer Galaxy, and the result is a power spectrum with exponent varying from cloud to cloud, in the range $1.72 < \beta < 2.9$, with a typical error of 0.08. The average exponent is $\beta = 2.1 \pm 0.3$ (Brunt 1999; Heyer 1999). This method has been calibrated

using stochastic fields (Stutzki et al. 1998), with purely random phases and no correlation between density and velocity. Correlations in real turbulent flows are likely to be important, and could affect the calibration of this method.

4. The PDF of Mass Density

The study of Probability Density Functions (PDF) in turbulent flows has received increasing attention over the last few years. PDFs can provide important information complementary to power spectra. They are also "easier" to use than power spectra, because they can be well defined at relatively low numerical resolution. A well known example of a combined use of power spectrum and PDF, limited to linear density fluctuations, is the Press–Shechter model of the galaxy mass distribution (Press & Schechter 1974).

A number of numerical studies have established that the PDF of mass density in isothermal turbulent flows is well approximated by a Log–Normal distribution (Vázquez-Semadeni 1994; Padoan, Nordlund & Jones 1997; Scalo et al. 1998; Passot & Vázquez-Semadeni 1998; Nordlund & Padoan 1999; Ostriker, Gammie & Stone 1999), which can be understood analytically (Nordlund & Padoan 1999). A highly radiative turbulent flow develops a complex system of interacting shocks that are able to fragment the mass distribution into a random network of dense cores, filaments and sheets and low density "voids", with a large density contrast of several orders of magnitude, depending on the size of the numerical mesh. The intermittent nature of the Log–Normal PDF of mass density means that most of the mass concentrates in a small fraction of the total volume of the simulation.

The Log–Normal distribution may be written as:

$$p(\log n')d\log n' = \frac{1}{(2\pi\sigma^2)^{1/2}} exp\left[-\frac{1}{2}\left(\frac{\log n' - \overline{\log n'}}{\sigma}\right)^2\right] d\log n' \tag{6}$$

where n' is the number density in units of the average density n_0,

$$n' = n/n_0, \tag{7}$$

the mean $\overline{\log n'}$ is determined by the standard deviation σ:

$$\overline{\log n'} = -\frac{\sigma^2}{2}, \tag{8}$$

which is found to be a function of the rms Mach number of the flow $\mathcal{M}$:

$$\sigma^2 = ln(1 + \mathcal{M}^2\beta^2) \tag{9}$$

or, for the linear density:

$$\sigma_{linear} = \beta \mathcal{M} \tag{10}$$

where $\beta \approx 0.5$, from numerical experiments. The standard deviation of the linear density distribution grows linearly with the rms Mach number of the flow (Nordlund & Padoan 1999; Ostriker, Gammie & Stone 1999).

5. The Mass Distribution of Dense Cores

In this section we derive the mass distribution of dense cores based on the two assumptions that i) the power spectrum of turbulence is a power law and ii) the typical size of a dense core scales as the thickness of the postshock gas.

If the typical size of a dense core is comparable to the thickness of the postshock gas, λ (§ 2), its mass m is:

$$m \sim \rho_1 \lambda^3 = \rho_0 \mathcal{M}_a \left(\frac{L}{\mathcal{M}_a} \right)^3 = \frac{\rho_0 L^3}{\mathcal{M}_a^2}, \tag{11}$$

where we have used the jump conditions (1) and (2). Equation (11) shows that on a given scale L, the mass of dense cores is proportional to the total mass available ($\rho_0 L^3$) divided by the second power of the Mach number on that scale ($\mathcal{M}_a^2$).

Given the power spectrum (5), the rms velocity, σ_v on the scale L is

$$\sigma_v \propto L^\alpha, \tag{12}$$

where

$$\alpha = \frac{\beta - 1}{2}. \tag{13}$$

The typical shock velocity on the scale L is therefore $\sigma_v(L)$, and the shock Mach number is given by (4), where v is replaced by $\sigma_v(L)$. Substituting this scale dependent expression of $\mathcal{M}_a$ into (11) one obtains

$$m \approx \frac{\rho_0 L_0^3}{\mathcal{M}_{a,0}^2} \left(\frac{L}{L_0} \right)^{4-\beta}, \tag{14}$$

where L_0 is the (large) scale where the turbulent velocity is v_0 and the rms Mach number is $\mathcal{M}_{a,0}$.

The smallest scale where significant density fluctuations may be expected is approximately the scale where the Mach number is of order unity:

$$m_{min} \approx \frac{\rho_0 L_0^3}{\mathcal{M}_{a,0}^{6/(\beta-1)}} \tag{15}$$

In MCs with a mass $M_0 = \rho_0 L_0^3 = 10^4$ M$_\odot$ a typical value of the Mach number is $\mathcal{M}_{a,0} \sim 10$. We then obtain $m_{min} \sim 0.0003$ M$_\odot$, for $\beta = 1.8$.

If L_0 in equation (14) is defined as the largest scale of the turbulent flow (the scale of turbulent energy injection), and we take $L = L_0$, we obtain an estimate of the mass of the largest cores formed by turbulent fragmentation,

$$m_{max} \approx \frac{\rho_0 L_0^3}{\mathcal{M}_{a,0}^2}, \tag{16}$$

where $\mathcal{M}_{a,0}$ is the rms Mach number on the largest turbulent scale. In MCs with a mass $M_0 = \rho_0 L_0^3 = 10^4$ M$_\odot$ and Mach number $\mathcal{M}_{a,0} = 10$, $m_{max} \sim 100$ M$_\odot$.

When deriving the distribution of core masses that results from super–sonic turbulence it is useful to consider the setup and interpretation of numerical experiments. Numerical turbulence experiments are in a certain sense scale–free; the density is usually rescaled so that the average density $\langle \rho \rangle = 1$ and the size of the box is scaled so that $L = 1$. The only distinguishing, scale dependent properties that remain after such scalings are the (sonic and Alfvénic) Mach numbers; from Larson's relations (Larson 1981) we expect larger scales to correspond to larger rms Mach numbers.

Even those relations are only statistical; we are allowed to consider two experiments with identical initial conditions (also with respect to Mach numbers and average gas density), but interpreted at different scales L_1, and $L_2 > L_1$. The total mass in the "large scale" experiment is obviously $(L_2/L_1)^3$ larger than in the "small scale" experiment. The cores in the large scale experiment would be equal in number, but heavier by the ratio $(L_2/L_1)^3$ than cores in the small scale experiment. On the other hand, the total number of cores in the small scale experiment is $(L_2/L_1)^3$ larger than in the large scale experiment, if the same total mass is used in the two cases (that is if cores from a number $(L_2/L_1)^3$ of small scale experiments are counted together). The result is therefore a total number of cores that depends on scale as:

$$N \propto L^{-3} \tag{17}$$

If there were no dependence of Mach numbers on scale, one would thus expect equal mass contributions from each logarithmic interval (IMF slope -1), as also shown by Elmegreen (1997) [3].

When the Mach number dependence on scale is taken into account the result is that the larger scales contribute relatively less, because of the scaling relation (14). Combining the relations (14) and (17) we

[3]Elmegreen (1997) also shows that this result does not depend on the fractal dimension of the self–similar distribution.

obtain:

$$N(m)\mathrm{d}\log m \propto m^{-3/(4-\beta)}\mathrm{d}\log m. \tag{18}$$

If the spectral index is consistent with the observed velocity dispersion–size Larson relation (Larson 1981) and with our preliminary numerical results (Boldyrev, Nordlund & Padoan 2001), then $\beta = 1.74$ and the mass distribution is

$$N(m)\mathrm{d}\log m \propto m^{-1.33}\mathrm{d}\log m, \tag{19}$$

which is almost identical to the Salpeter stellar IMF (Salpeter 1955).

6. The Mass Distribution of Collapsing Cores

The mass distribution of dense cores has been computed assuming that the pre–shock density is n_0 and the postshock density $\mathcal{M}_a n_0$, where $\mathcal{M}_a$ is scale dependent. A more precise computation should include the effect of the probability distribution of the value of $\mathcal{M}_a$ at each scale, or the overall effect of the statistics of the turbulent velocity field, which is the generation of a Log–Normal PDF of mass density (see § 4). This is necessary to compute the fraction of dense cores that are gravitationally unstable and collapse into protostars, since dense cores can be significantly denser than their average density predicted by the scaling laws. While most of the large cores will be dense enough to collapse, the probability that small cores are dense enough to collapse is determined by the PDF of mass density. Because of the intermittent nature of the Log–Normal PDF, even very small (sub–stellar) cores have a finite chance to be dense enough to collapse.

We write the thermal Jeans' mass as:

$$m_J = m_{J,0}\left(\frac{n}{n_0}\right)^{-1/2} \tag{20}$$

where:

$$m_{J,0} = 1.2\,m_\odot \left(\frac{T}{10K}\right)^{3/2}\left(\frac{n_0}{1000cm^{-3}}\right)^{-1/2} \tag{21}$$

is the Jeans' mass at the mean density n_0. The distribution of the Jeans' mass is obtained from the PDF of density as in Padoan, Nordlund & Jones (1997):

$$p(m_J)d\log m_j = \frac{1}{\sqrt{2\pi}\,\sigma/2}\left(\frac{m_J}{m_{J,0}}\right)^{-2} exp\left[-\frac{1}{2}\left(\frac{\log m_J - A}{\sigma/2}\right)^2\right] d\log m_J, \tag{22}$$

where m_J is in solar masses, and:

$$A = \log m_{J,0}^2 - \overline{\log n'} \tag{23}$$

The fraction of cores of mass m with gravitational energy in excess of their thermal energy is given by the integral of $p(m_J)$ from 0 to m. The mass distribution of collapsing cores is therefore

$$N(m)d\log m \propto m^{-3/(4-\beta)} \left[\int_0^m p(m_J)dm_J\right] d\log m \tag{24}$$

The mass distribution is plotted in Figure 3, for $\beta = 1.8$. In the top panel the mass distribution is computed for three different values of the largest turbulent scale L_0, assuming Larson type relations (Larson 1981). The mass distribution is a power law, determined by the power spectrum of turbulence, for masses larger than approximately 1 $m_\odot$. At smaller masses the mass distribution flattens, reaches a maximum at a fraction of a solar mass, and then decreases with decreasing stellar mass. Collapsing sub–stellar masses are found, thanks to the intermittent density distribution in the turbulent flow. The middle and bottom panel of Figure 3 show the dependence of the mass distribution on the rms Mach number of the flow and on the average gas density respectively.

The magnetic critical mass is derived in the next section. We have not used it here to obtain the mass distribution of collapsing cores because the thermal Jeans's mass is a more strict condition for collapse. The magnetic critical mass depends on the core morphology in relation to the field geometry and on the magnetic field strength that correlates with the gas density with a very large scatter (see below). It is possible therefore that magnetic pressure support against the gravitational collapse affects the shape of the mass distribution, but only as a secondary effect.

7. The Stellar IMF

Observations show that the stellar IMF is a power law above 1–2 $m_\odot$, with exponent around the Salpeter value $x = 1.35$, roughly independent of environment (Elmegreen 1998, 2000), gradually flattens at smaller masses, and peaks at approximately 0.2–0.6 $m_\odot$ (Hillenbrand 1997; Bouvier et al. 1998; Luhman 1999; Luhman & Rieke 1999; Luhman 2000; Luhman et al. 2000). The shape of the IMF below 1–2 $m_\odot$, and particularly the relative abundance of brown dwarfs, may depend on the physical environment (Luhman 2000).

The scalings discussed above result in a mass distribution of dense cores consistent with the stellar IMF for masses larger than 1 $m_\odot$, without invoking a sampling rate proportional to the free fall time, or "competition for mass" as in Elmegreen (1997, 1999). Two conclusions are possible; either there are effects in addition to those considered by Elmegreen, and they all happen to cancel each other, or else additional

effects are not important in the first place. In the spirit of Occam, let's consider the latter possibility. If, as argued elsewhere by Elmegreen (2000a), star formation essentially happens in a crossing time, then we may indeed see only one generation of stars being produced at each scale, rather than the repeated process implied by scaling with the local dynamical time. The picture thus is one where a particular MC forms as a consequence of the random intersection of counter-streaming, super–sonic motions (Ballesteros–Paredes, Hartmann & Vázquez–Semadeni 1999), internal turbulence creates the distribution of core masses derived above, and the cores are then grabbed by gravitation to form one generation of stars. Energy feedback from stars subsequently disperses the cloud before the process has time to repeat.

In the process envisaged above, turbulent fragmentation is responsible for creating the core mass distribution, while gravity is only responsible for the collapse of each protostar. The flattening and the turn around of the IMF is also easily accounted for in such a model. While scale–free turbulence generates a power law mass distribution down to very small masses, only cores with a gravitational binding energy in excess of their magnetic and thermal energy can collapse. The shape of the stellar IMF is then determined by the PDF of gas density, that is by the probability of small cores to be dense enough to collapse. The mass distribution of collapsing cores derived in the previous section and based on the Log–Normal PDF of mass density is indeed consistent with the observed IMF.

The approximate mass value where the IMF peaks can be derived without a knowledge of the PDF of mass density, using the scaling laws and the definition of the critical mass for collapse. We first consider the magnetic critical mass,

$$m_B = m_{B,0} \left(\frac{B}{B_0}\right)^3 \left(\frac{n}{n_0}\right)^{-2}, \tag{25}$$

where $m_{B,0}$ is the magnetic critical mass at the average number density n_0,

$$m_{B,0} = 8.3\mathrm{M}_\odot \left(\frac{B_0}{8\mu\mathrm{G}}\right)^3 \left(\frac{n_0}{10^3\mathrm{cm}^{-3}}\right)^{-2}, \tag{26}$$

(McKee et al. 1993). Padoan & Nordlund (1999) have shown that super–sonic and super–Alfvénic turbulence generates a correlation between gas density and magnetic field strength, consistent with the observational data. The two most important properties of such a B–n relation are the very large scatter, and the power law upper envelope ($B \propto n^{0.4}$). More recently, Padoan et al. (2001b) have computed the magnetic field strength in dense cores produced in numerical simulations of self–gravitating, super–sonic and super–Alfvénic turbulence. They found typical field strength as a function of column density in agreement with new compilations of observational samples by Crutcher (1999) and Bourke et al. (2000). Here we

adopt the following empirical B–n relation consistent with our previous works:

$$B = B_0 \left(\frac{\rho}{\rho_0} \right)^{0.5}, \tag{27}$$

where the exponent is 0.5, and not 0.4 as reported above, because we now refer to the average values of B inside bins of n, and not to the upper envelope of the B–n relation, as above.[4] We find the critical mass by imposing $m = m_B$, where m is given by equation (14), and m_B by equation (25),

$$m_{c,B} = m_{B,0} \left(\frac{\rho L_0^3}{m_{J,0}} \right)^{(\beta-1)/(15-3\beta)} \mathcal{M}_{a,0}^{-2/(5-\beta)}, \tag{28}$$

For $\beta = 1.8$, we get

$$m_c \approx m_{B,0} \mathcal{M}_{a,0}^{-0.625}. \tag{29}$$

The critical mass is therefore typically a few times smaller than the critical mass at the average density. For $\mathcal{M}_{a,0} = 10$, $n_0 = 10^3$ cm^{-3} and $B_0 = 8$ μG, the critical mass is approximately 2 m$_\odot$.[5] The probability that cores smaller than this mass are larger than their critical mass decreases with decreasing core mass, which could produce some flattening of the stellar IMF. Because of the large scatter in the B–n relation the magnetic critical mass does not define a sharp cut-off in the IMF, but rather a gradual flattening. A sharper mass scale is defined by the Jeans' mass in the cores,

$$m_{c,J} \approx m_{J,0} \mathcal{M}_{a,0}^{-2/(5-\beta)}, \tag{30}$$

where $m_{J,0}$ is the Jeans' mass at the average density defined in (21). For $\mathcal{M}_{a,0} = 10$, $n_0 = 500$ cm^{-3}, $T_0 = 10$ K and $\beta = 1.8$, the thermal critical mass is approximately 0.4 m$_\odot$. Therefore, using physical parameters typical of nearby molecular clouds, the present model predicts that the IMF should gradually flatten below approximately 2 m$_\odot$ and peak in a (logarithmic) neighborhood of 0.4 m$_\odot$, due to increasing thermal pressure support at smaller masses (cores smaller than their Jeans' mass are not included in the mass distribution).

This result is consistent with the analytic expression of the IMF derived in the previous section based of the density PDF. As can be seen in Figure 3, the IMF peaks at approximately 0.4 m$_\odot$, for $\mathcal{M}_{a,0} = 10$, $n_0 = 500$ cm^{-3}, $T_0 = 10$ K and $\beta = 1.8$.

---

[4]The slight steepening is due to the fact that the lower envelope of the B–n relation is steeper than the upper envelope.

[5]This value of $B_0 = 8$ μG provides a normalization of the B–n relation consistent with the results of our super-Alfvénic numerical simulations discussed in Padoan & Nordlund (1999) and in Padoan et al. (2001b).

7.1. The Largest Stellar Mass

In § 5 we have estimated the largest mass of dense cores formed by the process of turbulent fragmentation, given by the expression (16). The largest stellar mass should also be of the order of m_{max}. Assuming that the turbulent velocities are of the order of the virial velocities in the parent molecular cloud, and adopting the Larson relation $\rho_0 \propto L_0^{-1}$ (Larson 1981), we obtain $m_{max} \propto M_{cloud}^{0.5}$. This is very close to the empirical relation $m_{max} \propto M_{cloud}^{0.43}$ (Larson 1982), which is found for a cloud sample known to follow the above size–density relation. It is likely that the true exponent of this relation is slightly larger than the value found by Larson (1982), because the lifetime of the most massive stars is comparable to, or shorter than, the lifetime of their parent molecular clouds, and therefore the probability of observing the most massive stars decreases with increasing mass.

Elmegreen (1993, 1997) has argued that the largest stellar mass is related to the mass of the parent cloud for purely statistical reasons: the larger the cloud mass is, the higher the probability of populating the high mass tail of the IMF. Such a statistical argument is correct only if the normalization of the IMF is independent of the total cloud mass. The scalings derived above show that this is not the case; larger clouds in general have larger velocities and therefore form relatively fewer stars of a given mass. This is also indicated by observations, since it is commonly found that larger clouds have lower star formation efficiency than smaller clouds. However, since the star formation efficiency also depends on the low mass cut-off of the IMF, and since age differences also may enter, it would have been hard to draw firm conclusions from observations alone.

8. Discussion

We have found that the mass distribution of dense cores formed by turbulent fragmentation has a power law shape, with a slope consistent with the stellar IMF at intermediate and large masses. It is remarkable that the correct slope of the stellar IMF is obtained as a direct result of the power spectrum of super–sonic turbulence and the jump conditions for isothermal MHD shocks. There are no free parameters in this model, and provided that some general criteria are met, the slope of the stellar IMF is independent of the physical conditions in the star–forming clouds, as indicated by the observations (Elmegreen 1998, 2000).

We have also interpreted the gradual flattening of the IMF around 1–2 $M_\odot$ and its peak at

approximately 0.3–0.5 $M_\odot$ as the effect of thermal (possibly also magnetic) support against the gravitational collapse. The mass distribution of collapsing cores, computed on the basis of the PDF of mass density and the thermal Jeans' mass, is consistent with the observed stellar IMF, down to sub–stellar masses. We have shown that the IMF at low stellar masses is sensitive to the average physical properties of the star forming gas, such as the rms Mach number and the average gas density, also consistent with the observations (Luhman 2000).

Given the fact that turbulent fragmentation is unavoidable in super–sonic turbulence[6], and given the success of the present model in predicting the correct slope of the stellar IMF without any free parameter, it is difficult to argue that super–sonic turbulence does not play a dominant role in the generation of the stellar IMF. Other processes such as gravitational fragmentation (Larson 1973; Elmegreen & Mathieu 1983; Zinnecker 1984), opacity limited fragmentation (Hoyle 1953; Gaustad 1963; Yoneyama 1972; Suchkov & Shchekinov 1976; Low & Lynden-Bell 1976; Rees 1976; Yoshii & Saio 1985; Silk 1977a, b), protostar interactions and coagulation (Nakano 1966; Arny & Weissman 1973; Silk & Takahashi 1979; Bastien 1981; Yoshii & Saio 1985; Lejeune & Bastien 1986; Allen & Bastien 1995, 1996; Price & Podsiadlowski 1995; Murray & Lin 1996), stellar winds and outflows (Silk 1995; Nakano, Hasegawa & Norman 1995; Adams & Fatuzzo 1996), competitive accretion (Larson 1978; Tohline 1980; Bonnell et al. 1997; Myers 2000) must be relatively unimportant.

This conclusion is supported by a recent computation of the mass distribution of dense self–gravitating cores in numerical simulations of self–gravitating super–sonic MHD turbulence (Padoan et al. 2001b). The result is a power law mass distribution consistent with the stellar IMF. Mass distributions of cores from numerical simulations of super–sonic turbulence, consistent with the stellar IMF, are also reported by Klessen (2000).

For almost twenty years estimates of the mass distribution of dense cores in molecular clouds, based on molecular–line studies, found a shallow power law mass distribution with a single exponent in the range $0 < x < 0.7$[7], with a typical value $x = 0.5$. The main reasons for the shallow mass distribution

---

[6]This is true independently of the magnetic field strength, because super–sonic motions along the magnetic field always generate very strong compressions, even if the rms flow velocity is smaller than the Alfvén velocity.

[7](Myers, Linke & Benson 1983; Casoli, Combes & Gerin 1984; Blitz 1987; Carr 1987; Loren 1989; Stutzkie & Güsten 1990; Lada, Bally & Stark 1991; Nozawa et al. 1991; Tatematsu et al. 1993; Langer, Wilson & Anderson 1993; Williams & Blitz 1993; Blitz 1993; Williams et al. 1994; Williams, Blitz & Stark 1995;

obtained in these works are i) the relatively low density traced by the molecular emission lines normally used ($\sim 10^3$ cm^{-3} for ^{13}CO, and $\sim 10^4$ cm^{-3} for C^{18}O); ii) the limited density range probed by the same molecular emission lines; iii) the relatively low resolution that allows only the selection of large cores, with typical mass ranging from ≈ 10 m$_\odot$ to hundreds or thousands m$_\odot$. Clearly, cores selected in this way cannot be identified with single protostellar cores, as discussed in Padoan (1995), where it was predicted that the exponent of the intrinsic mass distribution of protostellar cores should have been $x > 1$, based on the stellar IMF. Recently, Onishi et al. (1999) have obtained a sample of dense cores in the Taurus molecular cloud complex using a higher density tracer, H^{13}CO$^+$, which probes a density of approximately $n = 10^5$ cm^{-3}. They found a power law mass distribution with exponent $x = 1.5 \pm 0.3$, in the mass range between 3.5 m$_\odot$ and 25 m$_\odot$. While most previous determinations of core mass distributions using molecular–line maps are affected by the arbitrary definition of an individual core, which is far from trivial in the hierarchical cloud structure, the dense H^{13}CO$^+$ cores found by Onishi et al. (1999) in Taurus are all very isolated and therefore unambiguously defined.

Recent dust continuum emission surveys, which also probe relatively high densities ($n = 10^5$–10^6 cm^{-3}), have provided more support to the idea that the stellar IMF reflects the mass distribution of dense cores. The mass distribution of dense cores in ρ Ophiuchi (Motte et al. 1998), and in the Serpens core (Testi & Sargent 1998), are found to be consistent with the stellar IMF. Motte et al. (1998) obtained a power law mass distribution with exponent $x = 1.5$ (in logarithmic units such that Salpeter's exponent is $x = 1.35$) in the range of masses between 0.5 m$_\odot$ and 3 m$_\odot$, and $x = 0.5$ in the range between 0.1 m$_\odot$ and 0.5 m$_\odot$. Testi & Sargent (1998) found $x = 1.1$, in the range of masses between 0.5 m$_\odot$ and 30 m$_\odot$.

9. Conclusions

In conclusion, we have related the stellar IMF to the mass distribution of dense cores formed by the process of turbulent fragmentation, assuming that only cores with gravitational energy in excess of their magnetic and thermal energy can collapse as protostars. Most sub–critical cores disperse back into the turbulent flow, and are therefore irrelevant for the process of star formation, as we have argued in other recent works (Padoan et al. 2001a, b). Previous theories of star formation (see Shu, Adams & Lizano 1987) assume that stars of small and intermediate mass are formed from sub–critical cores. In such theories,

---

Dobashi, Bernard & Fukui 1996; Onishi et al. 1996; Yonekura et al. 1997; Kawamura et al. 1998).

sub–critical cores are in static equilibrium and evolve quasi–statically, on the time–scale of ambipolar drift. We have argued that such a scenario is inconsistent with the turbulent nature of MCs (Padoan et al. 2001a, b).

We have derived the mass distribution of dense cores generated by the process of turbulent fragmentation, and have found a power law mass distribution consistent with the Salpeter stellar IMF, for stellar masses larger than 1–2 $m_\odot$. This result does not depend on any free parameters, unlike most previous theories of the stellar IMF, and it is the direct consequence of fundamental physical properties of super–sonic turbulence in MCs, such as the power spectrum of turbulence and the jump conditions for isothermal MHD shocks. We have also shown that another fundamental physical property of turbulent flows, namely the PDF of the gas density, can explain the shape of the IMF at smaller stellar masses, and the formation of gravitationally unstable cores of sub–stellar mass.

The main results of this work are: i) The power law stellar IMF at masses larger than 1–2 $m_\odot$ is the result of the self–similar nature of inertial range super–sonic turbulence; ii) The low mass roll-over and cut-off of the IMF is caused by the combined effects of the thermal support of the smallest cores against gravitational collapse and the density PDF of super–sonic turbulence; iii) The mass–scaling of the peak of the IMF may be expressed as a function of the physical parameters of turbulent star–forming clouds; primarily their rms turbulent velocity, size, temperature, magnetic field strength and average density; iv) For physical parameters typical of nearby MCs the peak of the IMF is predicted to be around 0.3–0.5 $m_\odot$; v) The slope of the IMF at masses larger than 1–2 $m_\odot$ is determined by the inertial range spectral index of super–sonic turbulence and the jump conditions for isothermal MHD shocks; vi) For magnetically dominated jump conditions, which are applicable to typical molecular cloud conditions, the IMF spectral index is equal to $3/(4-\beta)$, where β is the inertial range spectral index of super–sonic turbulence; vii) For a value of the inertial range spectral index $\beta = 1.74$, consistent with Larson's relations and with new numerical results, the IMF spectral index is $x = 1.33$, almost identical to Salpeter's slope.

We conclude that the process of turbulent fragmentation is essential to the origin of the stellar IMF, in support of the thesis that star formation can be viewed as the main consequence of the dissipation of super–sonic turbulence in molecular clouds.

We thank the anonymous referee for useful comments. We are grateful to Bruce Elmegreen, Alyssa Goodman, Chris McKee, Phil Myers and Ralph Pudritz for valuable discussions. This work was performed while PP held a National Research Council Associateship Award at the Jet Propulsion Laboratory,

California Institute of Technology. Å.N. acknowledges partial support by the Danish National Research Foundation through its establishment of the Theoretical Astrophysics Center.

References

Adams, F. C., Fatuzzo, M. 1996, ApJ, 464, 256

Allen, E. J., Bastien, P. 1995, ApJ, 452, 652

Allen, E. J., Bastien, P. 1996, ApJ, 467, 265

Arny, T., Weissman, P. 1973, AJ, 78, 309

Ballesteros-Paredes, J., Hartmann, L., Vázquez-Semadeni, E. 1999, ApJ, 527, 285

Bastien, P. 1981, A&A, 93, 160

Bazell, D., Désert, F. X. 1988, ApJ, 333, 353

Beech, M. 1987, Ap&SS, 133, 193

Blitz, L. 1987, in E. Morfill, M. Scholer (eds.), Physical Processes in Interstellar Clouds, p. 35

Blitz, L. 1993, in Protostars and Planets III, p. 125

Bourke, T., Myers, P., Robinson, G., Hyland, H. 2000, in preparation

Bouvier, J., Stauffer, J. R., Martin, E. L., Barrado y Navascues, D., Wallace, B., Bejar, V. J. S. 1998, A&A, 336, 490

Brunt, C. 1999, PhD Thesis, UMass

Brunt, C., Heyer, M. H. 2000, astro-ph/0011200

Burgers, J. M. 1974, in The Nonlinear Diffusion Equation, Reidel, Dordrecht

Carr, J. S. 1987, ApJ, 323, 170

Casoli, F., Combes, F., Gerin, M. 1984, A&A, 133, 99

Crutcher, R. M. 1999, ApJ, 520, 706

Dame, T. M., Elmegreen, B. G., Cohen, R. S., Thaddeus, P. 1986, ApJ, 305, 892

Dickman, R. L., M., M., Horvath, M. A. 1990, ApJ, 365, 586

Dobashi, K., Bernard, J., Fukui, Y. 1996, ApJ, 466, 282

Elmegreen, B. G. 1983, MNRAS, 203, 1011

Elmegreen, B. G. 1997, ApJ, 486, 944

Elmegreen, B. G. 1998, in M. Livio (ed.), Unsolved Problems in Stellar Evolution, Cambridge University Press, 59

Elmegreen, B. G. 1999, ApJ, 515, 323

Elmegreen, B. G. 2000, in T. M. . P. André (ed.), From Darkness to Light, ASP Conference Series

Elmegreen, B. G. 2000a, ApJ, 530, 277

Elmegreen, B. G. 2000b, MNRAS, 311, L5

Elmegreen, B. G., Falgarone, E. 1996, ApJ, 471, 816

Elmegreen, B. G., Mathieu, R. D. 1983, MNRAS, 203, 305

Falgarone, E., Phillips, T. G., Walker, C. 1991, ApJ, 378, 186

Falgarone, E., Puget, J. L., Pérault, M. 1992, A&A, 257, 715

Gaustad, J. E. 1963, ApJ, 138, 1050

Goodman, A. A., Barranco, J. A., Wilner, D. J., Heyer, M. H. 1998, ApJ, 504, 223

Gotoh, T., Kraichnan, R. H. 1993, Phys. Fluids, A, 5, 445

Heitsch, F., Mac Low, M. M. .and Klessen, R. S. 2000, astro-ph/0009227

Henriksen, R. N. 1986, ApJ, 310, 189

Henriksen, R. N. 1991, ApJ, 377, 500

Hetem, A., J., Lepine, J. R. D. 1993, A&A, 270, 451

Heyer, M. H. 1999, in J. Mangum, S. Radford (eds.), Imaging through Radio and Submm Wavelengths, 213

Heyer, M. H., Schloerb, F. P. 1997, ApJ, 475, 173

Hillenbrand, L. A. 1997, AJ, 113, 1733

Hobson, M. P. 1992, MNRAS, 256, 457

Hoyle, F. 1953, ApJ, 118, 513

Kawamura, A., Onishi, T., Yonekura, Y., Dobashi, K., Mizuno, A., Ogawa, H., Fukui, Y. 1998, ApJS, 117, 387

Kimura, T., Tosa, M. 1993, ApJ, 406, 512

Kleiner, S. C., Dickman, R. L. 1987, ApJ, 312, 837

Klessen, R. S. 2000, astro-ph/0011224

Klessen, R. S., Heitsch, F., Mac Low, M. 2000, ApJ, 535, 887

Kolmogorov, A. N. 1941, Dokl. Akad. Nauk. SSSR, 30, 301

Lada, E. A., Bally, J., Stark, A. A. 1991, ApJ, 368, 432

Langer, W. D., Wilson, R. W., Anderson, C. H. 1993, ApJ, 408, L45

Larson, R. B. 1973, MNRAS, 161, 133

Larson, R. B. 1981, MNRAS, 194, 809

Larson, R. B. 1982, MNRAS, 200, 159

Larson, R. B. 1992, MNRAS, 256, 641

Lee, S., Lele, S. K., Moin, P. 1991, Phys. Fluids A, 3, 657

Lejeune, C., Bastien, P. 1986, ApJ, 309, 167

Leung, C. M., Kutner, M. L., Mead, K. N. 1982, ApJ, 262, 583

Loren, R. B. 1989, ApJ, 338, 902

Low, C., Lynden-Bell, D. 1976, MNRAS, 176, 367

Luhman, K. L. 1999, ApJ, 525, 466

Luhman, K. L. 2000, astro-ph/0007059

Luhman, K. L., Rieke, G. H. 1999, ApJ, 525, 440

Luhman, K. L., Rieke, G. H., Young, E. T., Cotera, A. S., Chen, H., Rieke, M. J., Schneider, G., Thompson,

R. I. 2000, ApJ, 540, 1016

Mac Low, M. 1999, ApJ, 524, 169

Mac Low, M. ., Ossenkopf, V. 2000, A&A, 353, 339

Mac Low, M., Smith, M. D., Klessen, R. S., Burkert, A. 1998, Ap&SS, 261, 195

Mac Low, M.-M. 1998, in J. Franco, A. Carramiñana (eds.), Interstellar Turbulence, Cambridge University Press

Miesch, M. S., Bally, J. 1994, ApJ, 429, 645

Motte, F., Andre, P., Neri, R. 1998, A&A, 336, 150

Murray, S. D., Lin, D. N. C. 1996, ApJ, 467, 728

Myers, P. C. 1983, ApJ, 270, 105

Myers, P. C. 2000, ApJ, 530, L119

Myers, P. C., Linke, R. A., Benson, P. J. 1983, ApJ, 264, 517

Nakano, T. 1966, Prog. Theoret. Phys., 36, 515

Nakano, T., Hasegawa, T., Norman, C. 1995, ApJ, 450, 183

Nozawa, S., Mizuno, A., Teshima, Y., Ogawa, H., Fukui, Y. 1991, ApJS, 77, 647

Onishi, T., Mizuno, A., Kawamura, A., Fukui, Y. 1999, in Star Formation 1999, Proceedings of Star Formation 1999, held in Nagoya, Japan, June 21 - 25, 1999, Editor: T. Nakamoto, Nobeyama Radio Observatory, p. 153-158, p. 153

Onishi, T., Mizuno, A., Kawamura, A., Ogawa, H., Fukui, Y. 1996, ApJ, 465, 815+

Ostriker, E. C., Gammie, C. F., Stone, J. M. 1999, ApJ, 513, 259

Ostriker, E. C., Stone, J. M., Gammie, C. F. 2000, astro-ph/0008454

Padoan, P. 1995, MNRAS, 277, 377

Padoan, P., Bally, J., Billawala, Y., Juvela, M., Nordlund, Å. 1999, ApJ, 525, 318

Padoan, P., Jones, B., Nordlund, Å. 1997a, ApJ, 474, 730

Padoan, P., Juvela, M., Bally, J., Nordlund, Å. 1998, ApJ, 504, 300

Padoan, P., Juvela, M., Goodman, A. A., Nordlund, Å. 2001a, ApJ, (in press –also astro–ph/0011122)

Padoan, P., Nordlund, Å. 1997, astro–ph/9706176

Padoan, P., Nordlund, Å. 1999, ApJ, 526, 279

Padoan, P., Nordlund, Å., Jones, B. 1997b, MNRAS, 288, 145

Padoan, P., Nordlund, Å., Rögnvaldsson, Ö. E., Goodman, A. A. 2001b, ApJ, (submitted)

Padoan, P., Rosolowsky, E. W., Goodman, A. A. 2001c, ApJ, (in press –also astro–ph/0010344)

Padoan, P., Zweibel, E., Nordlund, Å. 2000, ApJ, 540, 332

Passot, T., Vázquez-Semadeni, E., A., P. 1995, ApJ, 455, 536

Passot, T. & Vázquez-Semadeni, E. 1998, Phys. Rev. E, 58, 4501

Price, N. M., Podsiadlowski, P. 1995, MNRAS, 273, 1041

Press, W. H. & Schechter, P. 1974, ApJ, 187, 425

Rees, M. J. 1976, MNRAS, 176, 483

Salpeter, E. E. 1955, ApJ, 121, 161

Sanders, D. B., Scoville, N. Z., Solomon, P. M. 1985, ApJ, 289, 372

Scalo, J. M. 1990, in R. Capuzzo-Dolcetta, C. Chiosi, A. D. Fazio (eds.), Physical Processes in Fragmentation and Star Formation, (Kluwer : Dordrecht, p.151

Scalo, J. M., Vázquez-Semadeni, E., Chappell, D., Passot, T. 1998, ApJ, 504, 835

Shu, F. H., Adams, F. C., Lizano, S. 1987, ARA&A, 25, 23

Silk, J. 1977a, ApJ, 214, 152

Silk, J. 1977b, ApJ, 214, 718

Silk, J. 1995, ApJ, 438, L41

Silk, J., Takahashi, T. 1979, ApJ, 229, 242

Stone, J. M., Ostriker, E. C., Gammie, C. F. 1998, ApJ, 508, L99

Stutzki, J., Bensch, F., Heithausen, A., Ossenkopf, V., Zielinsky, M. 1998, A&A, 336, 697

Stutzki, J., Güsten, R. 1990, ApJ, 356, 513

Suchkov, A. A., Shchekinov, I. A. 1976, Soviet Astronomy, 19, 403

Tatematsu, K., Umemoto, T., Kameya, O., Hirano, N., Hasegawa, T., Hayashi, M., Iwata, T., Kaifu, N., Mikami, H., Murata, Y., Nakano, M., Nakano, T., Ohashi, N., Sunada, K., Takaba, H., Yamamoto, S. 1993, ApJ, 404, 643

Testi, L., Sargent, A. I. 1998, ApJ, 508, L91

Vázquez-Semadeni, E. 1994, ApJ, 423, 681

Vázquez-Semadeni, E., Passot, T., Pouquet, A. 1996, ApJ, 473, 881

Vogelaar, M. G. R., Wakker, B. P. 1994, A&A, 291, 557

Ward-Thompson, D., Kirk, J. M., Crutcher, R. M., Greaves, J. S., Holland, W. S., André, P. 2000, astro-ph/0006069

Williams, J. P., Blitz, L. 1993, ApJ, 405, L75

Williams, J. P., De Geus, E. J., Blitz, L. 1995, ApJ, 428, 693

Williams, P. J., Blitz, L., Stark, A. A. 1995, in Astronomy Data Image Library, 01

Yonekura, Y., Dobashi, K., Mizuno, A., Ogawa, H., Fukui, Y. 1997, ApJS, 110, 21

Yoneyama, T. 1972, PASJ, 24, 87

Yoshii, Y., Saio, H. 1985, ApJ, 295, 521

Zimmermann, T., Stutzki, J., Winnewisser, G. 1992, in Evolution of Interstellar Matter and Dynamics of Galaxies, 254

Zinnecker, H. 1984, MNRAS, 210, 43

This manuscript was prepared with the AAS LaTeX macros v4.0.

Figure captions:

Figure 1: Mass distribution of gravitationally unstable cores from equation (24). Top panel: Mass distribution for different values of the largest turbulent scale L_0, assuming Larson type relations, $T_0 = 10$ K and $\beta = 1.8$. Middle panel: Mass distribution for different values of $\mathcal{M}_{a,0}$, assuming $n_0 = 500$ cm^{-3}, $T_0 = 10$ K and $\beta = 1.8$. Bottom panel: Mass distribution for different values of n_0, assuming $\mathcal{M}_{a,0} = 10$, $T_0 = 10$ K and $\beta = 1.8$. The mass distribution peaks at approximately 0.4 $m_\odot$, for the values $\mathcal{M}_{a,0} = 10$, $n_0 = 500$ cm^{-3}, $T_0 = 10$ K and $\beta = 1.8$, typical of nearby molecular clouds.

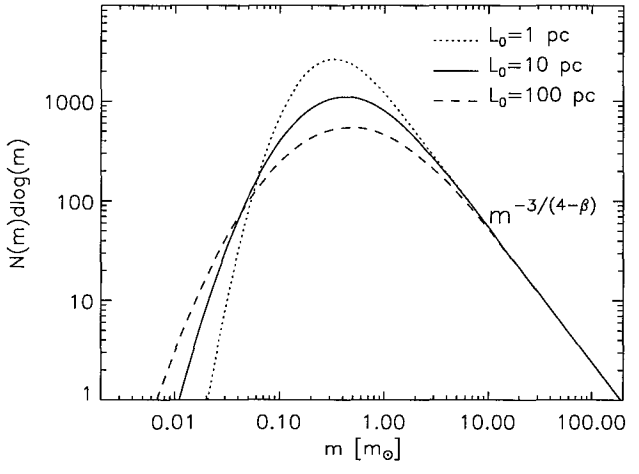
L0=1 pc
L0=10 pc
L0=100 pc
m^-3/(4-β)
N(m)dlog(m)
m [m⊙]
0.01
0.10
1.00
10.00
100.00
1
10
100
1000

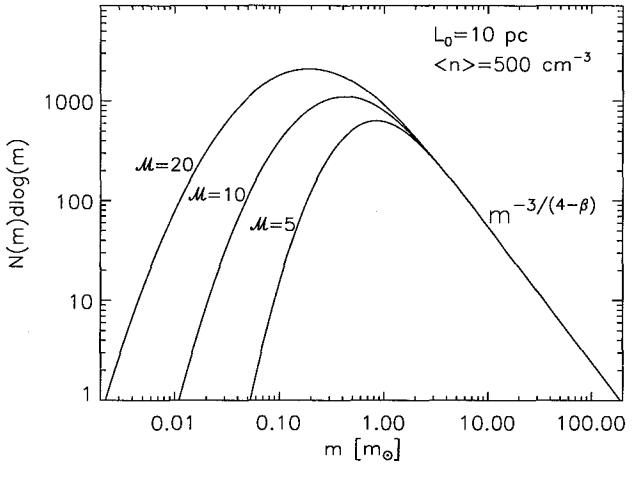
L0=10 pc
<n>=500 cm^-3
ℳ=20
ℳ=10
ℳ=5
m^-3/(4-β)
N(m)dlog(m)
m [m⊙]
0.01
0.10
1.00
10.00
100.00
1
10
100
1000

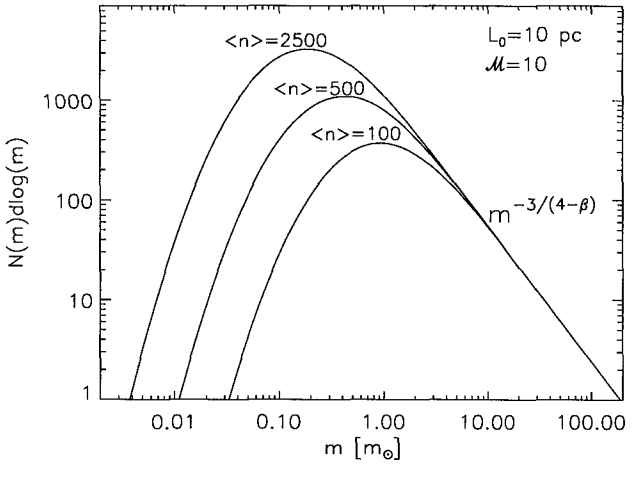
<n>=2500
<n>=500
<n>=100
L0=10 pc
ℳ=10
m^-3/(4-β)
N(m)dlog(m)
m [m⊙]
0.01
0.10
1.00
10.00
100.00
1
10
100
1000

Fig. 1.—